



OPEN

The role of implants and implant prostheses on the accuracy and artifacts of cone-beam computed tomography: an in-vitro study

Balwant Singh Gurjar, Vineet Sharma, Jyoti Paliwal[✉], Rajani Kalla, Kamal Kumar Meena & Mohammed Tahir

To assess the accuracy of CBCT in implant-supported prostheses and to evaluate metal artifacts with and without implants or implant prostheses. Accuracy and artifacts were assessed in the dried mandible at three points on the buccal and lingual cortical plates on the mandible's body near the crest and the base. On the buccal cortical plate, these points were labelled as A, B and C near the crest and D, E and F near the base of the body of the mandible. Similarly, points a to f were marked on the lingual cortical plate corresponding to points A to F. The study had two control groups, C0 for physical linear measurement (PLM) and C1 for radiographic linear measurement (RLM) and artifact assessment. There were seven test groups, TG 1 to 7, progressing from a single implant to implant full-arch prosthesis. For accuracy assessment, PLM was compared to RLM. CBCT artifacts were investigated in images integrated at 0.25 mm, 10 mm, and 20 mm at regions of interest on concentric circles at different intersecting angles by comparing grayscale values at C1 and TG1 to 7. The data were collected and statistically analyzed. A significant difference was observed between C0 and C1, and RLM in test groups at the superior axial plane. Similarly, PLM and test RLM in the sagittal plane at A-B, B-C, and D-E were statistically significant. A significant difference between PLM and RLM was also observed in the vertical plane at A-D, B-E, and C-F. Quantification of CBCT artifacts in the presence of implants or prostheses revealed that full-arch prostheses had the highest mean grayscale value, whereas single implants with a prosthesis had the lowest. The mean grayscale change was greatest around the implant and implant prosthesis. The mean grayscale value was maximum at 20 mm voxel integration scales (VIS) and lowest at 0.25 mm. CBCT is a clinically reliable device. Metal in implants or implant-supported prostheses prevents true assessment of the peri-implant area; therefore, lower VIS is suggested in the presence of implants or implant prostheses.

Radiological imaging has become increasingly important for diagnosis, clinical assessment, and treatment planning¹. In recent years, technology has advanced from two-dimensional conventional radiographs to three-dimensional digital imaging such as computed tomography (CT), magnetic resonance imaging (MRI), and cone-beam computed tomography (CBCT)².

CBCT is now an important part of diagnosis and treatment in fields like maxillofacial surgery, orthodontics, endodontics, implant planning, and evaluating patients after treatment³⁻⁷. Nevertheless, the presence of metals or alloys in implants, posts, cores, crowns, bridges, and amalgam fillings decreases image quality in the area adjacent to them due to reduced contrast caused by beam hardening, scattering effect, partial volume or edge effect, aliasing artifacts, and ring artifacts⁸⁻¹⁰. Due to increased life expectancy and the consequent increase in partial or complete edentulism, implant-supported prostheses have also grown in popularity¹⁰.

In their studies, Torres¹¹ and Shekhi¹² found the physical linear measurements to be more than radiographic CBCT measurements. Linear measurements of alveolar bone and maxillofacial structures by CBCT were proven accurate, trustworthy, and independent of the presence of dental implants by Ekrişh¹³ and Amarnath¹⁴. Beam

Department of Prosthodontics, RUHS College of Dental Sciences, Jaipur, India. ✉email: jyotishubh@yahoo.com

hardening artifacts were observed in the presence of metal implants in studies conducted by Schulze¹⁵ and Dreanert¹⁶.

The current study sought to evaluate the accuracy of CBCT as a measuring tool and quantify the artifact, if any, in the presence of implants and implant-supported prostheses by measuring and comparing linear distances in transverse, sagittal, and vertical planes in the physical model to radiographic measurements, as well as evaluating metal artifacts produced by CBCT of the mandible with or without implants or prostheses.

The null hypothesis stated that the accuracy of CBCT images is unaffected by the presence of implants and implant-supported prostheses.

Materials and methods

The research was conducted at the RUHS College of Dental Sciences in Jaipur, in the Department of Prosthodontics. The study received ethical committee clearance no. EC/PG-015/2019. The study used dry edentulous mandible and endosteal tapered SLA-treated (4×10 mm) titanium implants with titanium abutments (Superline Dentium implant system; Dentium South Korea). For assessment of accuracy, two points were marked on the buccal cortical plate of the body of a dried edentulous mandible, corresponding to the right mandibular canine (A and D) and mandibular first molar (C and F), both near the crest and base, respectively. Third point B and E were subsequently marked between points A and C and D and F respectively. Similarly, points a to f, corresponding to points A to F on the buccal cortical plate, were marked on the lingual cortical plate. This was referred to as 'Absolute Control (C0)' and was used for physical linear measurement (PLM). The radio-opaque gutta-percha balls of 0.5 mm diameter were then affixed using cyanoacrylate adhesive through points A to F and a to f on the buccal and lingual plates, respectively. This was referred to as radiographic control (C1), for radiographic linear measurements (RLM) in different spatial configurations. These reference points provide a standardized and reproducible framework for measuring and comparing PLM with RLM. The specific locations of the points were chosen to provide a reference for measurements in the transverse, sagittal, and vertical planes, which would be important for assessing the accuracy of CBCT images in the study (Figs. 1, 2).

Furthermore, seven test groups (TG1 to TG7) were created (Fig. 3). A styrofoam customized base was used to standardize the position of the mandible, with the base parallel to the horizontal plane and centered within the CBCT field of view (FOV). CBCT images were acquired using a CBCT machine (Care Stream CS3D-9000 machine; Care Stream Health Inc). The image volume was reconstructed with isotropic isometric $250 \times 250 \times 250$ μm voxels after receiving a scout image to include the region of interest.

Three independent observers performed PLM with a digital vernier caliper with a sensitivity of 0.01 mm. To determine dimensional accuracy, PLM was compared to RLM in all three planes: transverse, sagittal, and vertical.

RLM were performed in multi-planar oblique CBCT sections using the CBCT software measurement tool (Carestream 3D imaging, version 3.10.8; Carestream Health, Inc). RLM was performed on radiographic points in the transverse, sagittal, and vertical planes corresponding to physical points.

The artifacts were examined at locations A, B, a, and b in the superior axial plane. The images were integrated at a scale of 0.25 mm, 10.8 mm, and 21.8 mm and saved using the CBCT workplace screenshot tool. The

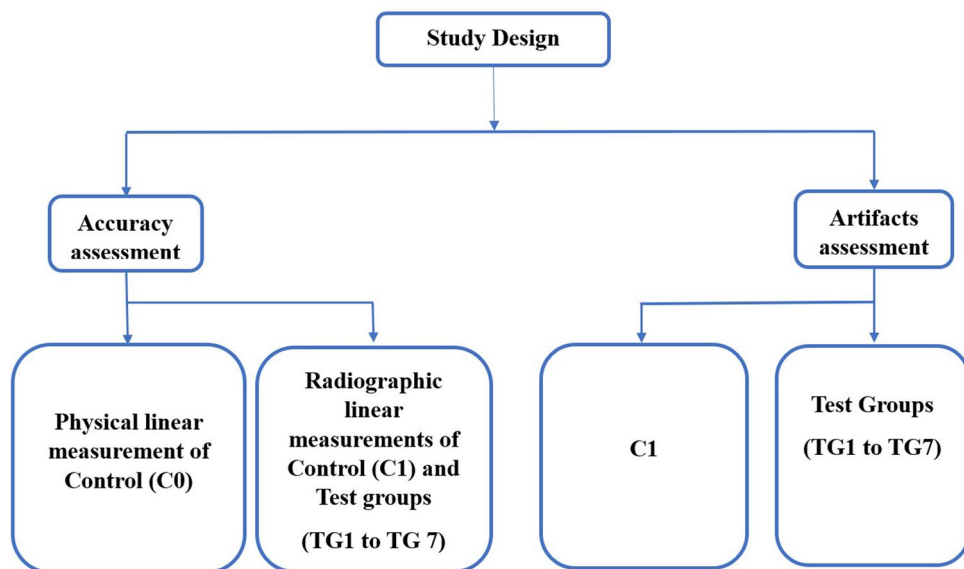


Figure 1. Flow-chart depicting the study design for assessment of dimensional accuracy and artifacts in CBCT at different stages. C0 = Absolute Control, C1 = Radiographic Control, TG1 = Single Implant placed at 43, TG2 = Implant-supported Porcelain fused to metal (PFM) crown with the abutment at 43, TG3 = Two Implants placed at 43 and 46, TG4 = Two Implant-supported PFM crowns at 43 and 46, TG5 = Implant-supported four-unit PFM prosthesis from 43 to 46, TG6 = Implant-supported four-unit PFM prostheses from 43 to 46 and 33 to 36 (Implants placed at 43, 46, 33 and 36), TG7 = Full arch implant-supported prosthesis.

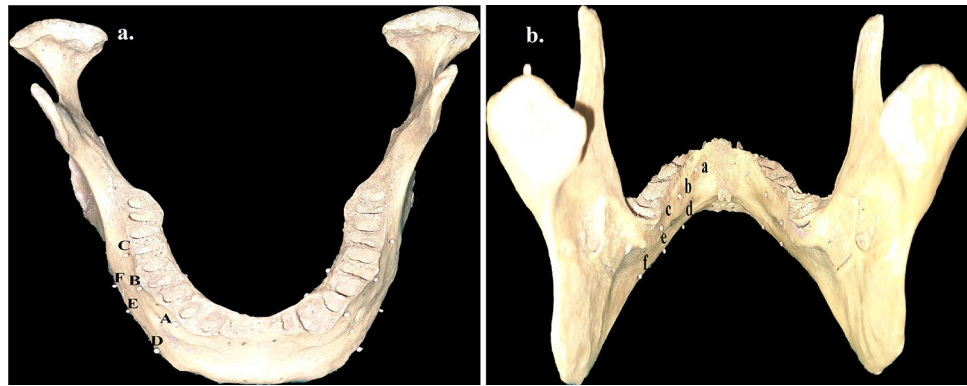


Figure 2. Reference points for accuracy measurement. (a) Buccal reference points for accuracy measurement at the crest of the mandible (A, B, C) and the base of the mandible (D, E, F). (b) Lingual reference points for accuracy measurement at the crest of the mandible (a, b, c) and the base of the mandible (d, e, f).

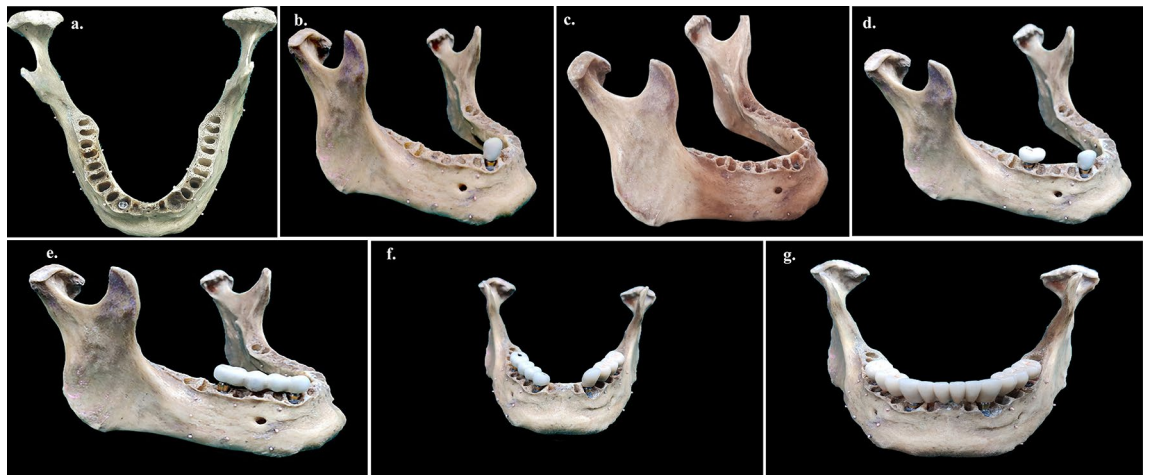


Figure 3. Stages of study model. (a) 4 × 10 mm titanium implant placed at 43 (TG1). (b) Implant-supported PFM crown with the abutment at 43 (TG2). (c) 4 × 10 mm titanium implants placed in the study model at 43 and 46 (TG3). (d) Implant-supported PFM single crowns at 43 and 46 (TG4). (e) Implant-supported four-unit PFM prosthesis from 43 to 46 (TG5). (f) Implant-supported four-unit PFM prostheses from 43 to 46 and 33 to 36 with 4 × 10 mm titanium implants placed in canine and first molar region bilaterally at 33, 43, 36, and 46 (TG6). (g) Full-arch implant-supported prosthesis (TG7).

screenshot was transformed to a 16-bit grayscale image using image software (The image J program, version 1.530; National Institute of Health and the Laboratory for Optical and Computational Instrumentation (LOCI)—University of Wisconsin) (grayscale range 0–255). Concentric circles with diameters of 6 mm, 10 mm, 15 mm, and 20 mm were drawn around the center of the implant at the canine and molar regions to define the region of interest. A reference line (Ro) was drawn across the center of the implant and parallel to the mandible's buccal and lingual cortical plates. Intersecting lines were made with respect to Ro at 0°, 65°, 90°, 115°, 180°, 245°, 270°, and 295°, intersecting the concentric circles to yield points of interest (Fig. 4). Macro (macro record tool of Image-J software version 1.530, National Institute of Health and the Laboratory for Optical and Computational Instrumentation (LOCI), University of Wisconsin) was used to delineate 32, 1-mm square regions of interest (ROI) for both implants placed at 43 and 46. Finally, the recorded Macro was run on an unmarked image to capture the average grayscale values of the square ROI mentioned previously (Figs. 5, 6). The artifacts in CBCT were recorded in the study at C1 and TG1 through TG7. The artifacts of the superior axial plane were then compared to those of the inferior axial plane (which corresponded to the appearance of the superior border of the mental foramen).

For osteotomy, conventional implant drilling protocols were followed for the Dentium surgical kit (SuperLine & Implantium Surgical Kit; Dentium). All Porcelain fused to metal (PFM) prostheses were fabricated by the lost wax technique using a base metal casting alloy.

The data obtained was compiled on an MS Office Excel sheet (v. 2016). The Statistical Package for the Social Sciences (SPSS) version 21.0 (IBM) was used to analyze the data. A one-way ANOVA test was used for inter-group comparison. The intra-group comparison was made using the post-hoc Tukey test. For all the statistical tests, $p < 0.05$ was considered statistically significant, keeping α error at 5% and giving 95% power to the study.

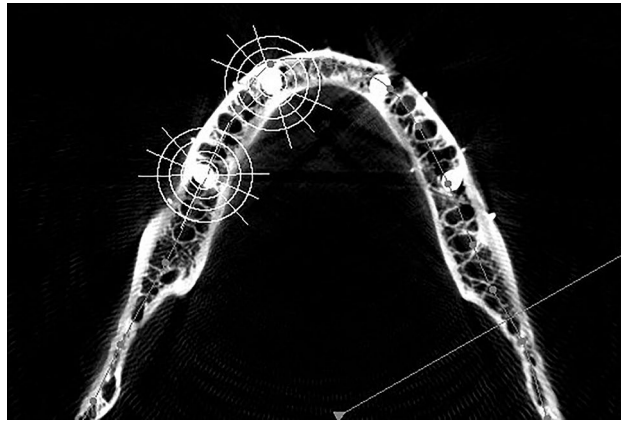


Figure 4. CBCT image depicting the region of interest for implant at canine and molar region.

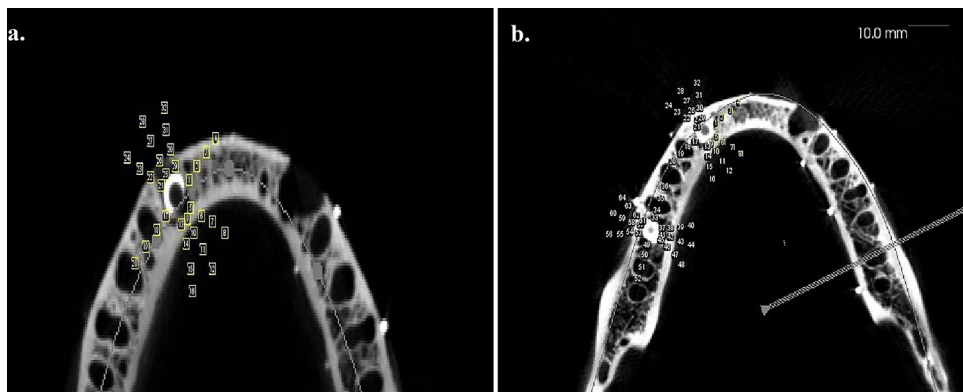


Figure 5. CBCT image depicting points ROI for the implant. (a) At canine (1–32). (b) At canine and molar region (1–64).

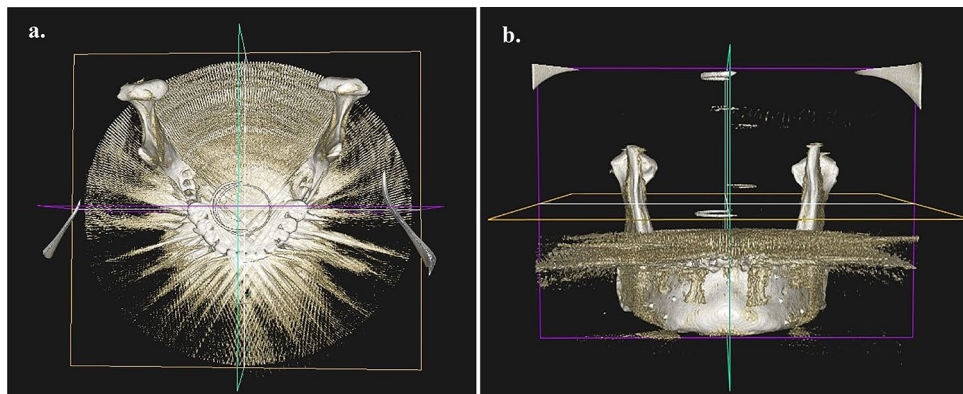


Figure 6. 3-D CBCT image showing artifacts with implants at 33, 36, 43, and 46 and full arch prosthesis. (a) Occlusal view. (b) Frontal view.

Results

The dimensional accuracy of CBCT as a measuring instrument was determined by comparing the RLM of C1 with the PLM (C0) in the transverse, sagittal, and vertical planes. The observed p -values after the paired t -test were statistically non-significant ($p > 0.05$) in all three planes.

In the transverse plane, the PLM (C0) was 9.23 mm, 10.77 mm, and 10.63 mm for A-a, B-b, and C-c in the superior plane, while the minimum and maximum RLM for test groups observed were 9.37 mm (TG1) and 9.63 mm (TG7), 10.57 mm (TG1) and 10.93 mm (TG6), and 9.37 mm (TG4 and TG5) and 10.73 mm (TG6) for A-a, B-b, and C-c, respectively. Similarly, PLM(C0) for D-d, E-e, and F-f in the inferior plane was 8.30 mm,

8.12 mm, and 7.19 mm, respectively, as compared to the observed minimum and maximum RLM values of 9.37 mm (TG1, TG4, and TG5) and 8.37 mm (TG7), 7.83 mm (TG5) and 8.03 mm (TG1 and TG7), 6.83 mm (TG7) and 7.13 mm (TG4 and TG5) for D-d, E-e, F-f thus, showing statistically significant results in the superior axial plane (Table 1).

The sagittal plane PLM for A-B, B-C, D-E, and E-F was 15.47 mm, 12.25 mm, 15.72 mm, and 10.83 mm, respectively, with minimum and maximum test group RLM values of 15.53 mm (TG4, TG6, and TG7) and 15.93 mm (TG5), 12.13 mm (TG4) and 12.27 mm (TG2), 16.03 mm (TG6) and 16.27 mm (TG3), 10.83 mm (TG6 and TG7) and 10.97 mm (TG1) for A-B, B-C, D-E, E-F. PLM and test RLM at A-B, B-C, and D-E in the sagittal plane were statistically significant ($p < 0.01$) (Table 2).

The vertical plane PLM (C0) for A-D, B-E, and C-F was 15.43 mm, 14.36 mm, and 15.35 mm, respectively, with a minimum and maximum value of test group RLM observed of 15.23 mm (TG1) and 15.63 mm (TG4, TG5, and TG7), 13.37 mm (TG6) and 14.33 mm (TG2, TG4, and TG5), 14.93 mm (TG4 and TG5), and 15.47 mm (TG1), respectively, for A-D, B-E, and C-F. There was a statistically significant difference between PLM and RLM at A-D, B-E, and C-F ($p < 0.01$) (Table 3). An intra-group analysis of test CBCT also revealed statistically significant differences across groups.

Quantification of artifacts of CBCT in the presence of implants or prostheses showed that with an increase in the number of implants or prostheses, the mean grayscale values increased. The highest mean grayscale value was seen in full-arch prostheses (170 ± 90.90), while the lowest grayscale value was seen in the single implant with prosthesis (98.03 ± 84.47) (Table 4). The mean grayscale change was greatest in the vicinity of the implant and implant prosthesis, with the greatest (64.64 ± 78.097) at 3 mm and the least (8.63 ± 81.269) at 10 mm (Table 5).

The canine and molar implant artifacts followed geometric distribution patterns. The grayscale changes at a 3 mm distance from the center of the canine implant (1 mm from the surface) had the highest values at 90° (94.33 ± 38.43) (lingual) and 270° (98.62 ± 41.722) buccally. Similarly, the highest grayscale values were observed around the molar implant at 90° (87.33 ± 49.808) and 270° (122.19 ± 74.682). In the region between canine and molar, reduced grayscale values were observed, i.e., at canine 180° (-17.14 ± 62.041) and molar 0° (-26.10 ± 61.173) due to the influence of implant or prosthesis (Table 6).

The grayscale changes at a 5 mm distance from the center of the canine implant had the highest values at 90° and 270° . The highest grayscale values were observed around the molar implant at 115° and 270° (Table 7).

The grayscale changes at a 7.5 mm distance from the center of the canine implant had the highest values at 115° and 270° . The highest grayscale values were observed around the molar implant at 90° and 270° (Table 8).

The grayscale changes at a 10 mm distance from the center of the canine implant had the highest values at 90° and 270° . The highest grayscale values were observed around the molar implant at 90° and 270° (Table 9).

In the region between canine and molar, reduced grayscale values were observed, i.e., at canine 180° and molar 0° due to the influence of implant or prosthesis (Tables 6, 7, 8, 9).

Grayscale and change in grayscale (ΔG) were evaluated at 0.25 mm, 10 mm, and 20 mm Voxel integration scale (VIS). The grayscale value increased at a VIS (10 mm and 20 mm), and statistically significant ($p < 0.01$) results were observed in mean grayscale and grayscale change (ΔG) at different VIS (Tables 10 and 11).

Discussion

The increasing dental awareness has led to increased implant-supported prostheses in partially and completely edentulous patients. The presence of dental implants and prostheses causes artifacts such as beam hardening, scattering, etc. These artifacts also reduce imaging diagnostic accuracy, making diagnosing peri-implant features difficult¹⁷. CBCT is a reliable radiographic tool with accuracy in the 0.163 mm to 0.40 mm range, as shown in our study. The results are supported by Maroua AL¹⁸, Ganguly R¹⁹, and Menezes et al.²⁰.

As we progressed from the single implant (TG-1) to full-arch implant-supported prosthesis (TG-7), the dimensional accuracy was reduced, confirming the co-relation between metal implants or implant-supported prostheses and the accuracy of CBCT image. The highly significant difference in observations can be explained by the role of artifacts induced by prostheses. The present study's findings prove that the artifacts increase as metal in implants and prostheses increases. An accurate delineation of buccal and lingual cortical plates in the peri-implant or prostheses area becomes difficult. The implant or prostheses produced artifacts strong enough to cause a dimensional error. This can be explained by the direction of the implant artifacts, which are diagonal to the implant axis, causing in-accuracies in transverse and sagittal planes making radiographic bone appearance wider than reality. This result is supported by Grobe A²¹, who, in an in-vivo study after placement of multiple implants, found a statistically highly significant (p value 0.003) difference between transverse measurements in CBCT and histological sections with a mean overestimation of 0.3 ± 0.04 mm in the CBCT image.

The TG RLM at the inferior axial plane showed no significant dimensional observation compared to C0. This can be explained by the reduced influence of prostheses as distance increases (at the inferior border). Studies have shown a sub-millimeter difference in CBCT measurements compared to the gold standard (caliper measurements)^{11,22,23–25}. The present study evaluated and compared measurements in all three planes, endorsing the conclusion that CBCT is a reliable diagnostic tool for linear measurements. However, previous studies focused on one or two implant configurations across multiple models, but none looked at the impact of prostheses on accuracy. The present study found that as we progressed from TG1 to TG 7, the dimensional accuracy of CBCT was reduced. As metals in implants and prostheses increase, accurate delineation of buccal and lingual cortical plates in the peri-implant and implant-supported prostheses area becomes difficult. Also, the artifacts increase in a direction diagonal to the implant axis, causing inaccuracies in transverse and sagittal planes making bone appear wider than reality, causing the dimensional error²¹.

Beam hardening is the most significant metal-induced artifact of CBCT, causing grayscale change^{8,26}. This is because lower energy X-ray beams from polychromatic X-rays are scattered and absorbed by denser metal and

| Test groups | N | Mean value (mm) | Standard deviation | Mean difference | Standard error | 95% confidence interval | | Significance |
|-------------|---|-------------------------|--------------------|-----------------|----------------|-------------------------|-------------|--------------|
| | | | | | | Lower bound | Upper bound | |
| A-a | | | | | | | | |
| C0 | 3 | 9.23 ^{ab} | 0.060 | | | | | |
| C1 | 3 | 9.37 | 0.060 | - 0.1333 | 0.0875 | - 0.44 | 0.173 | 0.009* |
| TG1 | 3 | 9.37 | 0.060 | - 0.1333 | 0.0875 | - 0.44 | 0.173 | |
| TG2 | 3 | 9.50 | 0.100 | - 0.2667 | 0.0875 | - 0.573 | 0.04 | |
| TG3 | 3 | 9.37 | 0.060 | - 0.1333 | 0.0875 | - 0.44 | 0.173 | |
| TG4 | 3 | 9.40 | 0.100 | - 0.1667 | 0.0875 | - 0.473 | 0.14 | |
| TG5 | 3 | 9.57 ^a | 0.210 | - 0.3333* | 0.0875 | - 0.64 | - 0.027 | |
| TG6 | 3 | 9.43 | 0.060 | - 0.2 | 0.0875 | - 0.507 | 0.107 | |
| TG7 | 3 | 9.63 ^b | 0.150 | - .4000* | 0.0875 | - 0.707 | - 0.093 | |
| B-b | | | | | | | | |
| C0 | 3 | 10.77 ^a | 10.770 | | | | | 0.000* |
| C1 | 3 | 10.78 ^b | 10.780 | - 0.00667 | 0.04869 | - 0.1773 | 0.1639 | |
| TG1 | 3 | 10.57 ^{abcdef} | 10.570 | 0.20333* | 0.04869 | 0.0327 | 0.3739 | |
| TG2 | 3 | 10.63 ^{ghij} | 10.630 | 0.13667 | 0.04869 | - 0.0339 | 0.3073 | |
| TG3 | 3 | 10.83 ^{ce} | 10.830 | - 0.06333 | 0.04869 | - 0.2339 | 0.1073 | |
| TG4 | 3 | 10.70 ^{kl} | 10.700 | 0.07 | 0.04869 | - 0.1006 | 0.2406 | |
| TG5 | 3 | 10.87 ^{dh} | 10.870 | - 0.09667 | 0.04869 | - 0.2673 | 0.0739 | |
| TG6 | 3 | 10.93 ^{eik} | 10.930 | - 0.16333 | 0.04869 | - 0.3339 | 0.0073 | |
| TG7 | 3 | 10.90 ^{fil} | 10.9 | - 0.13 | 0.04869 | - 0.3006 | 0.0406 | |
| C-c | | | | | | | | |
| C0 | 3 | 10.63 | 10.630 | | | | | 0.004 |
| C1 | 3 | 10.63 | 10.630 | 0 | 0.03852 | - 0.135 | 0.135 | |
| TG1 | 3 | 10.67 | 10.670 | - 0.03333 | 0.03852 | - 0.1683 | 0.1016 | |
| TG2 | 3 | 10.60 | 10.600 | 0.03333 | 0.03852 | - 0.1016 | 0.1683 | |
| TG3 | 3 | 10.67 | 10.670 | - 0.03333 | 0.03852 | - 0.1683 | 0.1016 | |
| TG4 | 3 | 10.57 ^{ab} | 10.570 | 0.06667 | 0.03852 | - 0.0683 | 0.2016 | |
| TG5 | 3 | 10.57 ^a | 10.570 | 0.06667 | 0.03852 | - 0.0683 | 0.2016 | |
| TG6 | 3 | 10.73 ^b | 10.730 | - 0.1 | 0.03852 | - 0.235 | 0.035 | |
| TG7 | 3 | 10.63 | 10.700 | - 0.06667 | 0.03852 | - 0.2016 | 0.0683 | |
| D-d | | | | | | | | |
| C0 | 3 | 8.300 | 0.020 | | | | | 0.356 |
| C1 | 3 | 8.230 | 0.060 | 0.06667 | 0.11235 | - 0.327 | 0.4603 | |
| TG1 | 3 | 8.130 | 0.060 | 0.16667 | 0.11235 | - 0.227 | 0.5603 | |
| TG2 | 3 | 8.200 | 0.100 | 0.1 | 0.11235 | - 0.2937 | 0.4937 | |
| TG3 | 3 | 8.170 | 0.060 | 0.13333 | 0.11235 | - 0.2603 | 0.527 | |
| TG4 | 3 | 8.130 | 0.060 | 0.16667 | 0.11235 | - 0.227 | 0.5603 | |
| TG5 | 3 | 8.130 | 0.060 | 0.16667 | 0.11235 | - 0.227 | 0.5603 | |
| TG6 | 3 | 8.300 | 0.000 | 0 | 0.11235 | - 0.3937 | 0.3937 | |
| TG7 | 3 | 8.370 | 0.380 | - 0.06667 | 0.11235 | - 0.4603 | 0.327 | |
| E-e | | | | | | | | |
| C0 | 3 | 8.12 | 0.03 | | | | | 0.051 |
| C1 | 3 | 8.07 | 0.06 | 0.05333 | 0.0743 | - 0.207 | 0.3137 | |
| TG1 | 3 | 8.03 | 0.06 | 0.08667 | 0.0743 | - 0.1737 | 0.347 | |
| TG2 | 3 | 7.93 | 0.06 | 0.18667 | 0.0743 | - 0.0737 | 0.447 | |
| TG3 | 3 | 7.97 | 0.06 | 0.15333 | 0.0743 | - 0.107 | 0.4137 | |
| TG4 | 3 | 7.97 | 0.06 | 0.15333 | 0.0743 | - 0.107 | 0.4137 | |
| TG5 | 3 | 7.83 | 0.21 | 0.28667* | 0.0743 | 0.0263 | 0.547 | |
| TG6 | 3 | 8 | 0.1 | 0.12 | 0.0743 | - 0.1403 | 0.3803 | |
| TG7 | 3 | 8.03 | 0.06 | 0.08667 | 0.0743 | - 0.1737 | 0.347 | |
| F-f | | | | | | | | |
| C0 | 3 | 7.19 ^{abcd} | 0.02 | | | | | 0.052 |
| C1 | 3 | 7.17 ^{efgh} | 0.12 | 0.02667 | 0.05009 | - 0.1488 | 0.2022 | |
| TG1 | 3 | 7.07 ⁱ | 0.06 | 0.12667 | 0.05009 | - 0.0488 | 0.3022 | |
| TG2 | 3 | 6.97 ^{ae} | 0.06 | 0.22667* | 0.05009 | 0.0512 | 0.4022 | |
| Continued | | | | | | | | |

| Test groups | N | Mean value (mm) | Standard deviation | Mean difference | Standard error | 95% confidence interval | | Significance |
|-------------|---|-----------------------|--------------------|-----------------|----------------|-------------------------|-------------|--------------|
| | | | | | | Lower bound | Upper bound | |
| TG3 | 3 | 6.93 ^{bijk} | 0.06 | 0.26000* | 0.05009 | 0.0845 | 0.4355 | |
| TG4 | 3 | 7.13 ^{ilm} | 0.06 | 0.06 | 0.05009 | - 0.1155 | 0.2355 | |
| TG5 | 3 | 7.13 ^{kno} | 0.06 | 0.06 | 0.05009 | - 0.1155 | 0.2355 | |
| TG6 | 3 | 6.90 ^{qin} | 0 | 0.29333* | 0.05009 | 0.1178 | 0.4688 | |
| TG7 | 3 | 6.83 ^{dhimo} | 0.06 | 0.36000* | 0.05009 | 0.1845 | 0.5355 | |

Table 1. Comparative assessment in transverse plane: A one-way ANOVA comparison followed by post-hoc Tukey HSD test. $p > 0.05$ statistically non-significant difference. * $-p < 0.05$ -statistically significant difference. The identical superscript indicates statistically significant difference amongst designated groups for respective linear measurement (eg. A-a, B-b...F-f).

even lighter titanium. In comparison, higher energy beams pass through the surface/body of the metal object and are recorded as a high-energy beam by the detector^{8,27}. Beam hardening causes metallic structure image distortion by differential absorption, known as a cupping artifact.

The lowest grayscale values observed in TG2 can be explained by the cupping effect, which is less with an 'only' implant (TG1) than for an implant with a prosthesis (TG2) (Table 10). The current study showed differential absorption of x-rays because of the metallic structure resulting in decreased grayscale values at the immediate periphery, as also shown by a study by Kou²⁸, who found the least grayscale value change in the proximity of a single dental implant prosthesis. The single implant with prostheses showed a higher decrease in grayscale values in the periphery than the only implant due to the additional cupping effect of increased metal content. Because of the artifact additive effect, the grayscale values increased with the number of implants^{8,28}.

Grobee A²¹ supports Benic GI⁹ fontanelle²⁹, who found significant artifacts up to 3.5 cm from the implant. The artifacts were present both in proximity and away from implants. The current results have emphasized the change in grayscale, with the diminishing influence of metal as the distance from the implant or prostheses increases.

The pattern of artifacts around the implant was observed at 3 mm, 5 mm, 7.5 mm, and 10 mm from the center of the implant, which showed a higher standard deviation at 0° and 180° in both the canine and molar region at 3 mm distance, indicating a greater amount of artifacts variation and worse image quality at these angular regions of interest (ROI)³⁰. Schulze⁸, Benic⁹, and Pauwels³¹ also found a similar decrease in grayscale values at the interproximal region between two implants or prostheses. Benic⁹ recorded the greatest grayscale change at points perpendicular to the mandibular axis, corroborating with the present study. While Benic⁹ found reduced grayscale values in mesial and distal regions of a single implant, the present study recorded negative grayscale changes in the interproximal area and distal to molar region, but not at 0° (mesial) in the canine region where only reduced grayscale change values were recorded. Also, a study by Pauwels R³¹ concluded that the area between two metal objects was most affected by artifacts, which concurs with the present study.

The mean grayscale change at the superior axial plane was higher (50.72) than at the inferior axial plane (33.36), indicating a greater influence of implant prosthesis. Likewise, the grayscale value increased at a higher VIS with significant observations in mean grayscale values and changes in grayscale values as a VIS indicator accuracy is proportional to VIS. The findings endorse previous observations of Candemill Ap³², who concluded that smaller voxel sizes were preferred for higher accuracy.

The present study revealed higher but statistically non-significant grayscale values when the canine region (126.04 ± 93.26) was compared with the molar region (120.17 ± 86.48). The results indicated that artifacts produced are independent of the area or place of implant or prosthesis placement. This result concurs with earlier studies by Benic GI⁹ and Fontenele²⁹, who also did not find any correlation between the position of the implant and artifacts.

The Limitation of the present study is a simplified in-vitro situation where the role of soft tissue around the mandible is eliminated. Since the study was carried out on a dry mandible, the reported results should be considered optimal, as precision and reliability are most likely lowered in clinical settings because of factors such as patient movement, adjoining soft tissue, and other intra-oral factors such as restorations that may influence linear measurements in a CBCT scan. Furthermore, lower VIS should be used to reduce artifacts and improve accuracy, as higher VIS increases artifacts. Moreover, the influence of different CBCT equipment/software for image reconstruction could also be studied.

Conclusion

The study aimed to assess the accuracy of CBCT as a measuring tool and quantify metal artifacts produced by CBCT of the mandible in the presence of implants and implant-supported prostheses. The results showed that the presence of implants and prostheses can cause artifacts, such as beam hardening and scattering, which can reduce the accuracy of the images. These artifacts were found to increase with the number of implants and the size of the prostheses. The artifacts were more pronounced in the presence of more metal, such as in full-arch implant-supported prostheses. The study also found that the artifacts were more pronounced in the superior axial plane than in the inferior axial plane. Furthermore, lower VIS should be used to reduce artifacts and improve accuracy, as higher VIS increases artifacts. Therefore, caution should be exercised when interpreting CBCT images with implants and prostheses, and additional diagnostic imaging modalities may be necessary to obtain more accurate information. Overall, this study provides important insights into the use of CBCT in

| Test groups | Mean | Standard deviation | F value | p-value |
|-------------|---------------------------|--------------------|---------|---------|
| A-B | | | | |
| C0 | 15.47 ^a | 0.12 | 17.443 | 0.000* |
| C1 | 15.13 ^{bdefgh} | 0.15 | | |
| TG1 | 15.70 ^{ab} | 0.10 | | |
| TG2 | 15.55 ^{ci} | 0.13 | | |
| TG3 | 15.63 ^{dj} | 0.06 | | |
| TG4 | 15.53 ^{ek} | 0.06 | | |
| TG5 | 15.93 ^{afijklgh} | 0.06 | | |
| TG6 | 15.53 ^g | 0.06 | | |
| TG7 | 15.53 ^h | 0.06 | | |
| B-C | | | | |
| C0 | 12.25 | 0.05 | 3.984 | 0.007* |
| C1 | 12.41 ^{ab} | 0.10 | | |
| TG1 | 12.30 | 0.10 | | |
| TG2 | 12.27 | 0.06 | | |
| TG3 | 12.17 ^a | 0.06 | | |
| TG4 | 12.13 ^b | 0.06 | | |
| TG5 | 12.23 | 0.06 | | |
| TG6 | 12.23 | 0.06 | | |
| TG7 | 12.23 | 0.06 | | |
| D-E | | | | |
| C0 | 15.72 ^{abcdefgh} | 0.08 | 6.695 | 0.000* |
| C1 | 16.16 ^a | 0.26 | | |
| TG1 | 16.23 ^b | 0.06 | | |
| TG2 | 16.25 ^c | 0.05 | | |
| TG3 | 16.27 ^d | 0.06 | | |
| TG4 | 16.23 ^e | 0.06 | | |
| TG5 | 16.27 ^f | 0.06 | | |
| TG6 | 16.03 ^g | 0.06 | | |
| TG7 | 16.07 ^h | 0.06 | | |
| E-F | | | | |
| C0 | 10.83 | 0.06 | 2.452 | 0.054 |
| C1 | 10.82 | 0.07 | | |
| TG1 | 10.97 | 0.06 | | |
| TG2 | 10.93 | 0.06 | | |
| TG3 | 10.90 | 0.00 | | |
| TG4 | 10.87 | 0.06 | | |
| TG5 | 10.87 | 0.06 | | |
| TG6 | 10.83 | 0.06 | | |
| TG7 | 10.83 | 0.06 | | |

Table 2. Comparative assessment in the sagittal plane: using one-way ANOVA test. $p > 0.05$ statistically non-significant difference. * $p < 0.05$ -statistically significant difference. The identical superscript indicates statistically significant difference amongst designated groups for respective linear measurement (eg. A-B, B-C...E-F).

| Groups | Mean measurements (mm) | Standard deviation | p-value |
|--------|--------------------------|--------------------|---------|
| A-D | | | |
| C0 | 15.43 | 0.15 | 0.003* |
| C1 | 15.43 | 0.06 | |
| TG1 | 15.23 ^{abc} | 0.06 | |
| TG2 | 15.43 | 0.21 | |
| TG3 | 15.53 | 0.12 | |
| TG4 | 15.63 ^a | 0.06 | |
| TG5 | 15.63 ^b | 0.06 | |
| TG6 | 15.53 | 0.06 | |
| TG7 | 15.63 ^c | 0.06 | |
| B-E | | | |
| C0 | 14.36 ^a | 0.08 | 0.000* |
| C1 | 14.40 ^b | 0.10 | |
| TG1 | 14.23 ^c | 0.06 | |
| TG2 | 14.33 ^d | 0.06 | |
| TG3 | 14.27 ^e | 0.06 | |
| TG4 | 14.33 ^f | 0.06 | |
| TG5 | 14.33 ^g | 0.06 | |
| TG6 | 13.37 ^{abcdefg} | 0.12 | |
| TG7 | 13.90 ^{abcdefg} | 0.00 | |
| C-F | | | |
| C0 | 15.35 ^{ai} | 0.06 | 0.000* |
| C1 | 15.45 ^{begj} | 0.17 | |
| TG1 | 15.47 ^{chk} | 0.12 | |
| TG2 | 15.37 ^{dl} | 0.06 | |
| TG3 | 15.17 | 0.15 | |
| TG4 | 14.93 ^{abcd} | 0.06 | |
| TG5 | 14.93 ^{ijkl} | 0.06 | |
| TG6 | 15.13 ^{ef} | 0.06 | |
| TG7 | 15.13 ^{gh} | 0.06 | |

Table 3. Comparative assessment in Vertical plane: using one-way ANOVA test. $p > 0.05$ statistically non-significant difference. * $p < 0.05$ -statistically significant difference. The identical superscript indicates statistically significant difference amongst designated groups for respective linear measurement (eg. A-D, B-E, and C-F).

| Groups | Mean ± SD | TG1 | TG2 | TG3 | TG4 | TG5 | TG6 | TG7 |
|---------|----------------|-------------------|-------|-------|-------|-------|-------|-------|
| | | Post Hoc p-values | | | | | | |
| Control | 86.33 ± 66.8 | 0.426 | 1.000 | 0.000 | 0.000 | 0.000 | 0.000 | 0.000 |
| TG1 | 101.41 ± 84.1 | 1 | | | | | | |
| TG 2 | 98.03 ± 84.47 | 1.000 | 1 | | | | | |
| TG3 | 119.68 ± 89.06 | 0.092 | 0.014 | 1 | | | | |
| TG4 | 123.66 ± 92.07 | 0.010 | 0.001 | 1.000 | 1 | | | |
| TG5 | 132.15 ± 85.36 | 0.000 | 0.000 | 1.000 | 1.000 | 1 | | |
| TG6 | 152.98 ± 89.68 | 0.000 | 0.000 | 0.000 | 0.000 | 0.000 | 1 | |
| TG7 | 170 ± 90.90 | 0.000 | 0.000 | 0.000 | 0.000 | 0.000 | 0.000 | 1 |

Table 4. Comparison of grayscale values of the test group. $p > 0.05$ statistically non-significant difference. $p < 0.05$ -statistically significant difference.

| Distance (mm) | Mean grayscale | Standard deviation | Standard error | p-value |
|---------------|----------------------|--------------------|----------------|---------|
| 3 mm | 64.64 ^{abc} | 78.097 | 3.013 | 0.000* |
| 5 mm | 51.55 ^{ade} | 75.977 | 2.931 | |
| 7.5 mm | 25.17 ^{bdf} | 79.199 | 3.055 | |
| 10 mm | 8.63 ^{cef} | 81.269 | 3.135 | |

Table 5. Mean grayscale change at various distances from the center of implant: a comparison using one-way ANOVA followed by post-hoc Tukey HSD test. $-\Delta G = G_{TG} - G_{CI}$. $p > 0.05$ statistically non-significant difference. * $-p < 0.05$ -statistically significant difference.

| 3 mm | Angular measurement | Mean | Standard deviation | Std. error | F | Significance |
|--------|---------------------|--------------------------|--------------------|------------|--------|--------------|
| Canine | 0 | 32.60 ^{abcdef} | 49.436 | 11.054 | 16.499 | 0.000* |
| Canine | 65 | 73.81 ^g | 39.615 | 8.645 | | |
| Canine | 90 | 94.33 ^{bh} | 38.435 | 8.387 | | |
| Canine | 115 | 81.19 ^{ci} | 37.237 | 8.126 | | |
| Canine | 180 | -17.14 ^{ghijkl} | 62.041 | 13.539 | | |
| Canine | 245 | 76.62 ^{dj} | 35.754 | 7.802 | | |
| Canine | 270 | 98.62 ^{ek} | 41.722 | 9.105 | | |
| Canine | 295 | 86.67 ^{fl} | 42.499 | 9.274 | | |
| Molar | 0 | -26.10 ^{abcdef} | 61.173 | 13.349 | 13.292 | 0.000* |
| Molar | 65 | 62.10 ^a | 55.994 | 12.219 | | |
| Molar | 90 | 87.33 ^{bh} | 49.808 | 10.869 | | |
| Molar | 115 | 59.71 ^{csi} | 56.162 | 12.255 | | |
| Molar | 180 | -9.10 ^{dghijkl} | 81.392 | 17.761 | | |
| Molar | 245 | 99.29 ^{ei} | 70.978 | 15.489 | | |
| Molar | 270 | 122.19 ^{fj} | 74.682 | 16.297 | | |
| Molar | 295 | 74.05 ^k | 60.918 | 13.293 | | |

Table 6. Mean grayscale change at 3 mm distance at various angular regions of interest: a one-way ANOVA comparison followed by post-hoc Tukey HSD test. $p > 0.05$ statistically non-significant difference. * $-p < 0.05$ -statistically significant difference. The identical superscript indicates statistically significant difference amongst designated groups for canine and molar.

| 5 mm | Angular measurement | Mean | Standard deviation | Std. error | F | P-value |
|--------|---------------------|-------------------------|--------------------|------------|--------|---------|
| Canine | 0 | 27.38 ^{ab} | 35.032 | 7.645 | 8.671 | 0.000* |
| Canine | 65 | 60.00 ^c | 55.987 | 12.217 | | |
| Canine | 90 | 68.62 ^d | 66.211 | 14.449 | | |
| Canine | 115 | 27.76 | 55.866 | 12.191 | | |
| Canine | 180 | -20.38 ^{cdef} | 60.955 | 13.302 | | |
| Canine | 245 | 58.05 | 65.218 | 14.232 | | |
| Canine | 270 | 79.33 ^{ae} | 31.696 | 6.917 | | |
| Canine | 295 | 79.14 ^{bf} | 40.768 | 8.896 | | |
| Molar | 0 | -10.52 ^{abcde} | 80.257 | 17.514 | 11.569 | 0.000* |
| Molar | 65 | 28.52 | 32.331 | 7.055 | | |
| Molar | 90 | 61.90 ^a | 35.148 | 7.670 | | |
| Molar | 115 | 70.19 ^{bf} | 42.621 | 9.301 | | |
| Molar | 180 | -14.90 ^f | 48.884 | 10.667 | | |
| Molar | 245 | 65.57 ^{cg} | 53.784 | 11.737 | | |
| Molar | 270 | 76.10 ^d | 48.131 | 10.503 | | |
| Molar | 295 | 68.33 ^{eg} | 46.167 | 10.075 | | |

Table 7. Mean grayscale change at 5 mm distance at various angular regions of interest: A one-way ANOVA comparison followed by post-hoc Tukey HSD test. $p > 0.05$ statistically non-significant difference. * $-p < 0.05$ -statistically significant difference. The identical superscript indicates statistically significant difference amongst designated groups for canine and molar.

| 7.5 mm | Angular measurement | Mean | Standard deviation | Std. error | F | Sig. |
|--------|---------------------|-------------------------|--------------------|------------|-------|--------|
| Canine | 0 | 31.10 | 50.773 | 11.080 | 1.464 | 0.184 |
| Canine | 65 | 31.86 | 55.408 | 12.091 | | |
| Canine | 90 | 34.90 | 56.508 | 12.331 | | |
| Canine | 115 | 42.86 | 69.749 | 15.220 | | |
| Canine | 180 | - 5.86 | 56.652 | 12.362 | | |
| Canine | 245 | 42.76 | 72.139 | 15.742 | | |
| Canine | 270 | 47.48 | 72.265 | 15.769 | | |
| Canine | 295 | 25.05 | 69.168 | 15.094 | | |
| Molar | 0 | - 15.67 ^{ad} | 50.019 | 10.915 | 4.894 | 0.000* |
| Molar | 65 | 33.71 ^a | 73.382 | 16.013 | | |
| Molar | 90 | 50.48 | 83.572 | 18.237 | | |
| Molar | 115 | 46.10 | 58.944 | 12.863 | | |
| Molar | 180 | - 21.48 ^{bcde} | 50.826 | 11.091 | | |
| Molar | 245 | 46.24 | 58.761 | 12.823 | | |
| Molar | 270 | 59.52 ^c | 75.221 | 16.415 | | |
| Molar | 295 | 50.19 ^c | 63.952 | 13.955 | | |

Table 8. Mean grayscale change at 7.5 mm distance at various angular regions of interest: A comparison using one-way ANOVA followed by post-hoc Tukey HSD test. $p > 0.05$ statistically non-significant difference. * - $p < 0.05$ -statistically significant difference. The identical superscript indicates statistically significant difference amongst designated groups for molar.

| 10 mm | Angular measurement | Mean | Standard deviation | Std. error | F | Sig. |
|--------|---------------------|------------------------|--------------------|------------|--------|--------|
| Canine | 0 | 16.33 | 33.900 | 7.398 | 8.786 | 0.000* |
| Canine | 65 | 24.71 | 53.446 | 11.663 | | |
| Canine | 90 | 32.81 | 53.479 | 11.670 | | |
| Canine | 115 | 20.48 | 58.644 | 12.797 | | |
| Canine | 180 | - 29.24 ^{abc} | 56.235 | 12.272 | | |
| Canine | 245 | 59.52 ^a | 90.882 | 19.832 | | |
| Canine | 270 | 65.81 ^b | 89.932 | 19.625 | | |
| Canine | 295 | 54.90 ^c | 85.537 | 18.666 | | |
| Molar | 0 | - 7.86 | 53.448 | 11.663 | 16.499 | 0.000* |
| Molar | 65 | 37.76 | 74.759 | 16.314 | | |
| Molar | 90 | 44.38 | 73.354 | 16.007 | | |
| Molar | 115 | 17.00 | 66.799 | 14.577 | | |
| Molar | 180 | - 8.14 | 46.654 | 10.181 | | |
| Molar | 245 | 17.43 | 107.206 | 23.394 | | |
| Molar | 270 | 50.29 | 72.613 | 15.845 | | |
| Molar | 295 | 45.71 | 81.668 | 17.821 | | |

Table 9. Mean grayscale change at 10 mm distance at various angular regions of interest: a one-way ANOVA comparison followed by post-hoc Tukey HSD test. $p > 0.05$ statistically non-significant difference. * - $p < 0.05$ -statistically significant difference. The identical superscript indicates statistically significant difference amongst designated groups for canine.

| Groups | Mean | Standard deviation | p-value |
|---------|---------------------|--------------------|---------|
| 0.25 mm | 83.79 ^a | 80.86 | 0.000* |
| 10 mm | 134.20 ^a | 89.50 | |
| 20 mm | 151.33 ^a | 85.33 | |

Table 10. Mean grayscale at different voxel integration scales (VIS): a one-way ANOVA comparison followed by post-hoc Tukey HSD test. The identical superscript indicates statistically significant difference amongst designated groups. (*- $p < 0.05$ -statistically significant difference)

| Groups | Mean | Standard deviation | Standard error | F | p-value |
|---------|--------------------|--------------------|----------------|-------|---------|
| 0.25 mm | 31.26 ^a | 81.507 | 2.723 | 5.450 | 0.004* |
| 10 mm | 37.27 | 81.892 | 2.736 | | |
| 20 mm | 43.96 ^a | 81.026 | 2.707 | | |

Table 11. Mean grayscale change(ΔG) at different integration scales (VIS): A one-way ANOVA comparison followed by post-hoc Tukey HSD test. – $\Delta G = G_{TG} - G_{CI}$, $p > 0.05$ statistically non-significant difference. * $-p < 0.05$ -statistically significant difference. The identical superscript indicates statistically significant difference amongst designated groups.

implant dentistry and highlights the need for further research to improve imaging quality and reduce artifacts in CBCT images.

Data availability

All data generated or analysed during this study are included in its [supplementary information](#) files.

Received: 21 June 2023; Accepted: 3 January 2024

Published online: 06 January 2024

References

- Danforth, R. A. Cone beam volume tomography: A new digital imaging option for dentistry. *J. Calif. Dent. Assoc.* **31**, 814–815 (2003).
- Shah, N., Bansal, N. & Logani, A. Recent advances in imaging technologies in dentistry. *World J. Radiol.* **6**, 794–807 (2014).
- Hendrikx, A. W., Maal, T., Dieleman, F., Van Cann, E. M. & Merckx, M. A. Cone-beam CT in the assessment of mandibular invasion by oral squamous cell carcinoma: Results of the preliminary study. *Int. J. Oral Maxillofac. Surg.* **39**, 436–439 (2010).
- Closmann, J. J. & Schmidt, B. L. The use of cone beam computed tomography as an aid in evaluating and treatment planning for mandibular cancer. *J. Oral Maxillofac. Surg.* **65**, 766–771 (2007).
- Tyndall, D. A. & Rathore, S. Cone-beam CT diagnostic applications: Caries, periodontal bone assessment, and endodontic applications. *Dent. Clin. N. Am.* **52**, 825–841 (2008).
- Mozzo, P., Procacci, C., Tacconi, A., Martini, P. T. & Andreis, I. A. A new volumetric CT machine for dental imaging based on the cone-beam technique: Preliminary results. *Eur. Radiol.* **8**, 1558–1564 (1998).
- Scarfe, W. C. Imaging of maxillofacial trauma: Evolutions and emerging revolutions. *Oral Surg. Oral Med. Oral Pathol. Oral Radiol. Endod.* **100**, S75–96 (2005).
- Schulze, R. *et al.* Artefacts in CBCT: A review. *Dentomaxillofac. Radiol.* **40**, 265–273 (2011).
- Benic, G. I., Sancho-Puchades, M., Jung, R. E., Deyhle, H. & Hämmerle, C. H. In vitro assessment of artifacts induced by titanium dental implants in cone beam computed tomography. *Clin. Oral Implants Res.* **24**, 378–383 (2013).
- Lee, M. Y., Song, K. H., Lee, J. W., Choe, B. Y. & Suh, T. S. Metal artifacts with dental implants: Evaluation using a dedicated CT/MR oral phantom with registration of the CT and MR images. *Sci. Rep.* **9**, 754 (2019).
- Torres, M. G., Campos, P. S., Segundo, N. P., Navarro, M. & Crusó-Rebello, I. Accuracy of linear measurements in cone beam computed tomography with different voxel sizes. *Implant Dent.* **21**, 150–155 (2012).
- Sheikhi, M., Dakhil-Ali, M. & Bahreinian, Z. Accuracy and reliability of linear measurements using tangential projection and cone beam computed tomography. *Dent. Res. J.* **12**, 271–277 (2015).
- Al-Ekrish, A. A. Comparative study of the accuracy of CBCT implant site measurements using different software programs. *Saudi Dent. J.* **33**, 355–361 (2021).
- Amarnath, G. S. *et al.* Comparison of cone beam computed tomography, orthopantomography with direct ridge mapping for pre-surgical planning to place implants in cadaveric mandibles: An ex-vivo study. *J. Int. Oral Health* **7**, 38–42 (2015).
- Draenert, F. G., Coppenrath, E., Herzog, P., Müller, S. & Mueller-Lisse, U. G. Beam hardening artefacts occur in dental implant scans with the NewTom cone beam CT but not with the dental 4-row multidetector CT. *Dentomaxillofac. Radiol.* **36**, 198–203 (2007).
- Chen, L. C., Lundgren, T., Hallström, H. & Cherel, F. Comparison of different methods of assessing alveolar ridge dimensions prior to dental implant placement. *J. Periodontol.* **79**, 401–405 (2008).
- Schulze, R. K., Berndt, D. & d’Hoedt, B. On cone-beam computed tomography artifacts induced by titanium implants. *Clin. Oral Implants Res.* **21**(1), 100–7 (2010).
- Maroua, A. L., Ajaj, M. & Hajeer, M. Y. The accuracy and reproducibility of linear measurements made on CBCT-derived digital models. *J. Contemp. Dent. Pract.* **17**, 294–299 (2016).
- Ganguly, R., Ramesh, A. & Pagni, S. The accuracy of linear measurements of maxillary and mandibular edentulous sites in cone-beam computed tomography images with different fields of view and voxel sizes under simulated clinical conditions. *Imaging Sci. Dent.* **46**, 93–101 (2016).
- Menezes, C. C., Janson, G., da Silveira, M. C., Cambiagli, L. & Garib, D. G. Precision, reproducibility, and accuracy of bone crest level measurements of CBCT cross sections using different resolutions. *Angle Orthod.* **86**, 535–542 (2016).
- Gröbe, A. *et al.* Accuracy of bone measurements in the vicinity of titanium implants in CBCT data sets: A comparison of radiological and histological findings in minipigs. *Biomed. Res. Int.* **2017**, 3848207 (2017).
- Bohner, LOL., Tortamano, P., Marotti, J. Accuracy of linear measurements around dental implants by means of cone beam computed tomography with different exposure parameters. *Dentomaxillofac. Radiol.* **46**(5), 20160377 (2017).
- Rokn, A. R. *et al.* Accuracy of linear measurements using cone beam computed tomography in comparison with clinical measurements. *J. Dent.* **13**, 333–339 (2016).
- Gerlach, N. L. *et al.* Reproducibility of 3 different tracing methods based on cone beam computed tomography in determining the anatomical position of the mandibular canal. *J. Oral Maxillofac. Surg.* **68**, 811–817 (2010).
- Luangchana, P., Pornprasertsuk-Damrongsri, S., Kiattavorncharoen, S. & Jirajariyavej, B. Accuracy of linear measurements using cone beam computed tomography and panoramic radiography in dental implant treatment planning. *Int. J. Oral Maxillofac. Implants* **30**, 1287–1294 (2015).
- De Man, B., Nuyts, J., Dupont, P., Marchal, G. & Suetens, P. Metal streak artifacts in X-ray computed tomography: A simulation study. *IEEE Trans. Nucl. Sci.* **46**, 691–696 (1999).

27. Miracle, A. C. & Mukherji, S. K. Conebeam CT of the head and neck, part 1: Physical principles. *AJNR Am. J. Neuroradiol.* **30**, 1088–1095 (2009).
28. Kuo, R. F., Fang, K. M., Ty, W. & Hu, C. Y. Quantification of dental prostheses on cone-beam CT images by the Taguchi method. *J. Appl. Clin. Med. Phys.* **17**, 207–220 (2016).
29. Fontenele, R. C., Nascimento, E. H., Vasconcelos, T. V., Noujeim, M. & Freitas, D. Q. Magnitude of cone beam CT image artifacts related to zirconium and titanium implants: Impact on image quality. *Dentomaxillofac. Radiol.* **47**, 20180021 (2018).
30. Terrabuio, B. R. *et al.* Cone-beam computed tomography artifacts in the presence of dental implants and associated factors: An integrative review. *Imaging Sci. Dent.* **51**, 93–106 (2021).
31. Pauwels, R. *et al.* Quantification of metal artifacts on cone beam computed tomography images. *Clin. Oral Implants Res.* **24**, 94–99 (2013).
32. Candemil, A. P. *et al.* Influence of voxel size on cone beam computed tomography artifacts arising from the exomass. *Oral Surg. Oral Med. Oral Pathol. Oral Radiol.* **132**, 456–464 (2021).

Author contributions

B.S.G.: conceptualization, software, formal analysis, data curation, writing—original draft, resources. V.S.: writing—resources, writing—original draft, writing—review and editing, formal analysis, supervision. J.P.: conceptualization, methodology, formal analysis, supervision, project administration, resources, writing—original draft, writing—review and editing. R.K., K.K.M., M.T.: supervision, visualization.

Competing interests

The authors declare no competing interests.

Additional information

Supplementary Information The online version contains supplementary material available at <https://doi.org/10.1038/s41598-024-51293-3>.

Correspondence and requests for materials should be addressed to J.P.

Reprints and permissions information is available at www.nature.com/reprints.

Publisher's note Springer Nature remains neutral with regard to jurisdictional claims in published maps and institutional affiliations.



Open Access This article is licensed under a Creative Commons Attribution 4.0 International License, which permits use, sharing, adaptation, distribution and reproduction in any medium or format, as long as you give appropriate credit to the original author(s) and the source, provide a link to the Creative Commons licence, and indicate if changes were made. The images or other third party material in this article are included in the article's Creative Commons licence, unless indicated otherwise in a credit line to the material. If material is not included in the article's Creative Commons licence and your intended use is not permitted by statutory regulation or exceeds the permitted use, you will need to obtain permission directly from the copyright holder. To view a copy of this licence, visit <http://creativecommons.org/licenses/by/4.0/>.

© The Author(s) 2024